

Published in final edited form as:

*Dev Dyn.* 2009 December ; 238(12): 3043–3055. doi:10.1002/dvdy.22139.

## Cyclic *Nrarp* mRNA Expression Is Regulated by the Somitic Oscillator but *Nrarp* Protein Levels Do Not Oscillate

David Wright<sup>#1</sup>, Zoltan Ferjentsik<sup>#1</sup>, Shang-Wei Chong<sup>2</sup>, Xuehui Qiu<sup>2</sup>, Jiang Yun-Jin<sup>2</sup>, Pascale Malapert<sup>3</sup>, Olivier Pourquié<sup>3</sup>, Nick Van Hateren<sup>4</sup>, Stuart A. Wilson<sup>4</sup>, Claudio Franco<sup>5</sup>, Holger Gerhardt<sup>5</sup>, J. Kim Dale<sup>1,‡</sup>, and Miguel Maroto<sup>1,‡,\*</sup>

<sup>1</sup>Division of Cell and Developmental Biology, College of Life Sciences, University of Dundee, Dundee, United Kingdom

<sup>2</sup>Laboratory of Developmental Signalling and Patterning, Genes and Development Division, Institute of Molecular and Cell Biology, Proteos, Singapore

<sup>3</sup>Howard Hughes Medical Institute, Stowers Institute for Medical Research, and Department of Anatomy and Cell Biology, University of Kansas School of Medicine, Kansas City, Missouri

<sup>4</sup>Department of Molecular Biology and Biotechnology, University of Sheffield, Sheffield, United Kingdom

<sup>5</sup>Vascular Biology Laboratory, London Research Institute-Cancer Research UK, London, United Kingdom

# These authors contributed equally to this work.

### Abstract

Somites are formed progressively from the presomitic mesoderm (PSM) in a highly regulated process according to a strict periodicity driven by an oscillatory mechanism. The Notch and Wnt pathways are key components in the regulation of this somitic oscillator and data from *Xenopus* and zebrafish embryos indicate that the Notch-downstream target *Nrarp* participates in the regulation of both activities. We have analyzed *Nrarp/nrarp-a* expression in the PSM of chick, mouse and zebrafish embryos, and we show that it cycles in synchrony with other Notch regulated cyclic genes. In the mouse its transcription is both Wnt- and Notch-dependent, whereas in the chick and fish embryo it is simply Notch-dependent. Despite oscillating mRNA levels, *Nrarp* protein does not oscillate in the PSM. Finally, neither gain nor loss of *Nrarp* function interferes with the normal expression of Notch-related cyclic genes.

### Keywords

*Nrarp*; Notch pathway; embryo; somitic oscillator; PSM; cyclic gene

### INTRODUCTION

Segmentation is a key feature of the body plan of all vertebrates, including humans, that initiates very early in embryonic development. The first sign of metamerism or segmentation is seen when vertebrate embryos develop somites, the precursors of several segmented

© 2009 Wiley-Liss, Inc.

\*Correspondence to: Division of Cell and Developmental Biology, University of Dundee, Dow St, Dundee DD1 5EH, UK.

m.maroto@dundee.ac.uk.

‡Drs. Dale and Maroto are joint senior authors.

organs such as the axial skeleton, body skeletal muscles, and part of the dermis. Somites are formed in a highly regulated process called somitogenesis from the unsegmented presomitic mesoderm, or PSM (Christ et al., 2007; Holley, 2007; Bryson-Richardson and Currie, 2008; Dequeant and Pourquié, 2008). During the formation of somites the most mature cells located at the rostral end of the PSM bud off as an epithelial sphere of cells to form the new somite. Somite formation occurs simultaneously with the recruitment of newly generated mesenchymal cells from the primitive streak/tail bud into the caudal region of the PSM (Bellairs, 1986; Selleck and Stern, 1991; Schoenwolf et al., 1992; Catala et al., 1995; Psychoyos and Stern, 1996; Sawada and Aoyama, 1999; Chuai and Weijer, 2008; Shook and Keller, 2008).

Critical molecular and embryological experimental data obtained in the last 10 years has shown that somitogenesis is governed by a molecular oscillator that drives cyclic expression of genes in the PSM and which is coupled to the formation of the somites (Cinquin, 2007; Holley, 2007; Dequeant and Pourquié, 2008). Expression of these cyclic genes is coordinated such that a wave of expression travels caudorostrally throughout the PSM during the formation of one somite. All cyclic genes identified to date encode either (a) components or modulators of the Notch pathway (Palmeirim et al., 1997; McGrew et al., 1998; Aulehla and Johnson, 1999; Holley et al., 2000; Jiang et al., 2000; Jouve et al., 2000; Leimeister et al., 2000; Bessho et al., 2001; Oates and Ho, 2002; Sieger et al., 2004; Shankaran et al., 2007), (b) components of the Wnt pathway (Aulehla et al., 2003; Ishikawa et al., 2004; Dale et al., 2006), or (c) components of the FGF pathway (Dale et al., 2006; Dequeant et al., 2006; Niwa et al., 2007).

*Nrarp* (Notch-regulated ankyrin-repeat protein) is a downstream target of the Notch signaling pathway expressed in the PSM and encodes a 114 amino acid protein that has a carboxy-terminal domain containing two ankyrin-repeat motifs (Krebs et al., 2001; Lamar et al., 2001; Pirot et al., 2004). The gene was initially isolated during a screen for developmentally expressed genes in *Xenopus* embryos (Gawantka et al., 1998). In vitro experiments have shown that *Nrarp* is able to form a ternary complex with Notch intracellular domain (NICD) and RBPj (Lamar et al., 2001). Its overexpression in *Xenopus* and zebrafish embryos blocks Notch activity by inhibiting NICD-mediated transcription by means of a completely unknown mechanism. The authors reported that ectopic *Nrarp* decreases NICD levels (Lamar et al., 2001; Ishitani et al., 2005) whereas morpholino treatment against *nrarp-a* stabilizes NICD (Ishitani et al., 2005), suggesting that the presence of *Nrarp* protein is related with NICD instability. In addition to this function in the Notch pathway, zebrafish *nrarp-a* stabilizes Lef1 protein, a pivotal transcription factor in the Wnt signaling cascade, by blocking its ubiquitination (Ishitani et al., 2005). Thus, *Nrarp*/*nrarp-a* could be a pivotal element connecting Notch and Wnt, the two major pathways implicated in the machinery of the segmentation clock in vertebrates. Here, we report that the expression of chick and mouse (Krebs et al., 2001) *Nrarp* and zebrafish *nrarp-a* (Topczewska et al., 2003) is dynamic in the PSM of the three species. The progression of *Nrarp* dynamic transcription is coincident with that of other cyclic genes of the Notch pathway, such as *Lunatic fringe* (*Lfng*) in chick and mouse or *deltaC* in zebrafish. Notably, the level of *Nrarp* protein does not oscillate in the chick PSM. *Nrarp* transcription is Notch-dependent but Wnt-independent in the chick and the fish embryo, whereas in the mouse embryo *Nrarp* is both Notch- and Wnt-dependent. Lastly, Notch regulated clock gene oscillations are unaffected in embryos lacking *Nrarp* function.

## RESULTS

### The Expression of *cNrarp* in the Early Chick Embryo

We analyzed the expression of *cNrarp* at the early stages of development of the chick embryo by in situ hybridization and observed that it is expressed in several tissues in which cellular differentiation is regulated by the Notch signaling pathway. *cNrarp* expression is detected from Hamburger and Hamilton (HH) stage 4 (Hamburger and Hamilton, 1951), where is restricted to the neural plate and mesoderm, similar to other members of the Notch pathways ( $n = 8$ ; Fig. 1A; data not shown). *cNrarp* is expressed very strongly in the unsegmented paraxial mesoderm at all the stages analyzed, but it is not present at all in the somites ( $n = 63$ ; Fig. 1B–E,G–H). In addition, it is clearly expressed in the intermediate mesoderm precursor of the mesonephric tubules (Fig. 1E), similar to the pattern of expression described for *mNrarp* in the mouse embryo (Krebs et al., 2001). *cNrarp* is clearly detected along the neural tube at the different stages analyzed and extends from the very caudal end rostrally to the head region (Fig. 1D–G). At HH stage 13 *cNrarp* is expressed in the otic vesicles and the entire brain region (Fig. 1F), similar to what has been described in the E8.75 mouse embryo (Krebs et al., 2001). At HH stage 21, there is strong signal in the lateral telencephalic vesicle, in the olfactory pits, the mesencephalon, the metencephalon at its rostral border, and the rhombencephalon, but expression seems to be weak or absent in the dorsal myelencephalic wall and the meso-diencephalic and meso-metencephalic folds (Fig. 1H).

### Dynamic Expression of *Nrarp* in the PSM

Dequeant and colleagues reported a microarray analysis performed with mouse PSM samples in which mouse *Nrarp* displayed an oscillatory profile (Dequeant et al., 2006). We decided to analyze the pattern of expression of *cNrarp* in the PSM of a large collection of HH stage 11–12 chick embryos carefully controlling the level of staining. Under these conditions, we found that indeed *cNrarp* displays different patterns in the PSM of a group of stage matched embryos. Some embryos displayed a broad caudal band of *cNrarp* extending across most of the PSM, while others showed a narrow rostral band at the level of presumptive somite  $S_{-1}$  that disappears at the level of the forming somite  $S_0$  ( $n = 84$ ; Fig. 2A–F). *cNrarp* transcripts seems to be more stable than those of other cyclic genes and if the staining is not properly controlled all the embryos display a quite similar staining pattern. This result suggests that the expression of *cNrarp* is dynamic in the chick PSM, similar to other cyclic genes belonging to the Notch signaling pathway. We also reexamined *Nrarp* in the mouse PSM by in situ hybridization on E9.5–E10.5 embryos ( $n = 35$ ) and observed different patterns of expression in the caudal PSM, indicative of its dynamic nature, similar to previous reports (Fig. 2G–K; Dequeant et al., 2006; Sewell et al., 2009). *mNrarp* can be observed mainly in two clear domains: a posterior domain that seems to be dynamic across the caudal and medial PSM, and an anterior domain, seen as a narrow stripe, that reaches the caudal half of the forming somite and disappears once the border is completed. Of interest, in the chick PSM the rostral band of expression of *Nrarp* is missing because its expression is down-regulated earlier, suggesting species-specific functions during the formation of the somitic border. Finally, we analyzed *Nrarp* expression in the zebrafish embryo, which express two isoforms, *nrarp-a* and *nrarp-b*, but only *nrarp-a* is expressed in the PSM (Topczewska et al., 2003). To verify if *nrarp-a* expression is dynamic we performed fluorescent double in situ hybridization ( $n = 37$ ) using probes for both *deltaC* (Fig. 3A1–G1), which is one of the cyclic genes characterized in the fish embryo (Jiang et al., 2000), and *nrarp-a* (Fig. 3A2–G2). We found that, although the stability of *nrarp-a* transcript makes the analysis more difficult, it is still nevertheless possible to observe that the front of progression of both genes is simultaneous and seems to progress from the caudal to the rostral end of the PSM (Fig. 3A3–G3). After the somite is formed, *nrarp-a* is still

maintained in the first two to three somites (Fig. 3A2–G2), which is different to the situation described above in chick and mouse embryos. In summary, these data clearly indicate that it is possible to observe different patterns of expression of *Nrarp* in the PSM of a variety of vertebrate embryos, suggesting that it is a conserved cyclic gene.

### ***Nrarp* Oscillates in Synchrony With the Notch-Dependent Cyclic Gene *Lfng***

To create a visual image representing the pattern of expression of *cNrarp* along one full cycle of oscillation, we analyzed a large set of stage-matched embryos ( $n = 84$ ) hybridized with an *Nrarp* riboprobe, as previously described for other cyclic genes (Dale et al., 2003; Maroto et al., 2005). The domains of expression and their distance from the last formed somite boundary were measured and the measurements for each individual embryo were plotted in order of the advancing anterior expression limit. These data clearly show that the mRNA expression profile of chick *Nrarp* sweeps the PSM caudorostrally in a progressive manner (Fig. 2L). The front of transcription progresses fast initially and then slows rostrally until it reaches the  $S_{-1}$  level, where *cNrarp* becomes down-regulated just before formation of the new somitic border begins. The main difference between the *cNrarp* expression profile and that of other Notch target clock genes analyzed in this way, such as *Hairy1*, *Hairy2*, and *Lfng* (Maroto et al., 2005), is the region corresponding to the degradation of transcripts, which in the case of *cNrarp* does not produce a clear dynamic profile. Instead, *cNrarp* seems to disappear gradually along the entire territory, suggesting that either *Nrarp* transcripts are more stable than those of other cyclic genes or its degradation is not regulated in the same way. In summary, the *cNrarp* expression profile is similar to other cyclic genes, although some differences exist, which are probably due to a longer half-life of its transcripts (see below).

We then performed *in vitro* experiments to confirm the nature of this dynamic expression. To that end we prepared half embryo cultures, in which the two halves of the PSM of HH stage 11–12 chick embryos ( $n = 9$ ) and E9.5–E10.5 mouse embryos ( $n = 10$ ) were processed independently, one half was fixed immediately and the other was cultured for defined periods of time. *In situ* hybridization analysis revealed that it is possible to detect different patterns of expression in the two chick and mouse PSM halves, demonstrating that the profile of *Nrarp* is dynamic, as expected for a cyclic gene (Fig. 4A,C). After 90 min, *cNrarp* completes a full oscillation and the two halves of the chick PSM displayed again the same pattern of expression with a new somite having formed in the cultured half ( $n = 7$ ; Fig. 4B). As expected, after treatment with cycloheximide the *cNrarp* signal is stronger in the treated side than in the control half, but the progression of *cNrarp* is not arrested ( $n = 12$ ; Fig. 4D), which is consistent with this expression profile being independent of new protein synthesis for one given cycle, as previously observed for other cyclic genes dependent upon Notch activity such as *cHairy1*, *cHey2*, and *cLfng* (Palmeirim et al., 1997; McGrew et al., 1998; Leimeister et al., 2000). We next used the half embryo culture system to determine whether *Nrarp* oscillates in synchrony with *Lfng* in the chick and mouse PSM (McGrew et al., 1998; Aulehla and Johnson, 1999). The results clearly show that in both HH stage 10–12 chick PSM ( $n = 19$ ) and embryonic day (E) 9.5–E10.5 mouse PSM ( $n = 35$ ) the front of progression of *Nrarp* is simultaneous with that of *Lfng* along the entire PSM, from the moment they start to be expressed at the caudal end until they reach the level of  $S_{-1}$  in the rostral PSM (Fig. 4E–L; Sewell et al., 2009). The main difference between the two patterns of expression seems to be related with the stability of the transcripts. As mentioned above, the regression of the caudal domain is not so clear with *Nrarp* because the transcripts appear to be more stable than those of *Lfng* (black brackets in Fig. 4G,H,K,L). In the rostral region, *cNrarp* but not *cLfng* is down-regulated before the formation of the new somite border (black arrowheads in Fig. 4E–H), whereas in the mouse embryo *mNrarp* and *mLfng* are co-expressed until the somite is formed (black arrowheads in Fig. 4I–L). In summary, the

results indicate that *Nrarp* is a cyclic gene that oscillates together with members of the Notch signaling pathway.

### Cyclic *Nrarp* Is Dependent on Wnt Signaling Activity in the Mouse but Not in the Chick or Fish Embryo

It is generally accepted that the somitic oscillator relies on two main components, the Notch and the Wnt signaling pathways, by controlling the expression of the cyclic genes (Cinquin, 2007; Holley, 2007; Dequeant and Pourquié, 2008). Because *Nrarp* progresses together with *Lfng* in chick and mouse, we first determined if the expression is Notch-dependent by treating the embryos in vitro with the  $\gamma$ -secretase inhibitor DAPT, a drug that has been extensively used to manipulate and inhibit the Notch pathway in numerous contexts (Dovey et al., 2001; Micchelli et al., 2003; Lewis et al., 2003; Morohashi et al., 2006), including that of somitogenesis (Dale et al., 2003; Horikawa et al., 2006; Mara and Holley, 2007; Riedel-Kruse et al., 2007; Ozbudak and Lewis, 2008; Gibb et al., 2009). When we cultured half of a chick PSM with 100  $\mu$ M DAPT, *cNrarp* was severely down-regulated in the PSM, whereas it was still detectable in the neural tube (n = 6; Fig. 5A). Similar treatment in mouse abrogated *mNrarp* in the PSM (n = 6; Fig. 5B), showing that in both species *Nrarp* in the PSM is Notch-dependent. We repeated the experiment using a second Notch-blocking drug, LY411575, which also acts to inhibit the  $\gamma$ -secretase enzymatic complex (Lanz et al., 2004), and the results were identical (n = 7 and n = 10; data not shown). This result is consistent with previous observations indicating that *Nrarp* is seriously compromised in *Hes7*, *Notch1*, *Delta1*, and *Delta3* homozygous null mouse embryos (Krebs et al., 2001; Sewell et al., 2009; Ferjentsik et al., 2009). Similarly, we found that *nrarp-a* is severely down-regulated in the PSM of *aei/deltaD* (n = 26) or *des/notch1a* (n = 19) mutant zebrafish embryos (Fig. 5E–G). These results demonstrate that *Nrarp/nrarp-a* expression is dependent upon Notch activity in the PSM of the three species analyzed.

We next examined if *Nrarp* is dependent upon Wnt activity. To that end, we repeated the same kind of assay treating the samples with 200  $\mu$ M CKI-7, an inhibitor of the Wnt pathway (Peters et al., 1999; McKay et al., 2001) recently used to investigate the specific function of the Wnt pathway in the machinery of the somitic oscillator (Gibb et al., 2009). When we cultured half of a HH stage 10–12 chick PSM with CKI-7, expression of the Wnt target gene *Lef1* was abolished (n = 5; data not shown; Gibb et al., 2009). However, after this treatment, *cNrarp* was maintained in the PSM with a pattern similar to the untreated half (n = 8; Fig. 5C), suggesting that chick *Nrarp* dynamic expression is not Wnt-dependent, at least during this treatment period. A similar result was observed with *nrarp-a* in zebrafish embryos after exposure to CKI-7 (n = 30; Fig. 5H,I). However, the results of CKI-7 treatment were different using samples prepared from E9.5–E10.5 mouse embryos, because under these conditions, expression of *mNrarp* was lost entirely (n = 11; Fig. 5D). These results indicate that, whereas the expression of *Nrarp* in the PSM of the chick and fish embryo is Notch-dependent and Wnt-independent, in the mouse embryo its expression is dependent upon both Notch and Wnt.

### *Nrarp* Protein Level Does Not Oscillate in the Chick PSM

We then tested if *Nrarp* protein was expressed dynamically along the PSM. Using the chick full-length polypeptide we prepared a specific anti-*Nrarp* antibody that after affinity purification recognized a protein of approximately 15–17 kDa molecular weight, as judged by Western blot analysis with samples prepared from PSM. The antibody recognized endogenous *Nrarp* (n = 15) and ectopic *Nrarp* expressed in electroporated chick embryos (n = 8) by Western blot analysis (Fig. 6A), but unfortunately it did not yield reproducible results by immunohistochemistry (data not shown). We thus analyzed *Nrarp* protein levels in the chick PSM using a similar approach to one we have used previously to evaluate cLfng

(Dale et al., 2003). In this analysis, one half of the embryonic sample was used to perform in situ hybridization using a *cLfng* probe, and the second half was further dissected to isolate the caudal half of the PSM. This tissue was then either used to generate protein sample to be analyzed by Western blot or to generate cDNA for quantitative real-time polymerase chain reaction (qRT-PCR) analysis (Fig. 6B). We decided to evaluate the levels of Nrarp protein in different samples from distinct phases of an oscillation using *cLfng* as a reference for the oscillation phase in each sample because the profile of *cNrarp* transcripts is not as clear as that of *cLfng*, as indicated previously. Nevertheless, using this experimental design we confirmed by qRT-PCR that the ratio of *Nrarp* mRNA vs. *GAPDH* mRNA varies significantly between samples at different phase of the oscillation cycle, as expected for a cyclic gene ( $n = 20$ ; Fig. 6C). Surprisingly, when we performed Western blot analysis using the anti-Nrarp antibody, we detected that cNrarp protein was expressed with similar intensity in the PSM samples irrespective of the phase of the oscillation cycle, as judged by the *cLfng* pattern of expression ( $n = 72$ ; Fig. 6B). We also confirmed that the ratio of Nrarp protein vs.  $\alpha$ -Tubulin protein did not change between different samples ( $n = 27$ ; Fig. 6C). Thus, we can conclude that the level of Nrarp protein produced by the cyclic gene *Nrarp* does not oscillate in the chick PSM.

To test if the profile of expression of Nrarp mRNA and protein could be related to their prolonged stability compared with that of another cyclic component such as *Lfng*, we evaluated both *Lfng* and Nrarp mRNA and protein after a timed inhibition of Notch signaling ( $n = 54$ ). We observed that after 2 hr exposure to DAPT *Lfng* mRNA, as evaluated by in situ hybridization, is completely lost in the PSM whereas *Nrarp* mRNA degradation is only starting to be evident, although there is still a significant amount of transcripts (Fig. 6D,E,I,J). *Nrarp* mRNA degradation continues over the time course and all transcripts have degraded after 16 hr (Fig. 6K,L). Similarly, Nrarp protein level, as evaluated from samples prepared by Western blot (see the Experimental Procedures section), remains unchanged 4 hr after treatment with DAPT, by which time *Lfng* protein level is already barely observed ( $n = 32$ ; Fig. 6H). These results indicate that the half life of Nrarp mRNA and protein are longer than those of *Lfng*, which we think it could contribute to the differences observed in its profile of expression compared with other cyclic genes.

### Neither Gain Nor Loss of Nrarp Function Interferes With the Normal Expression of Notch-Related Cyclic Genes

We next evaluated the effect of ectopic Nrarp on the expression of Notch-regulated cyclic genes. To that end, we misexpressed Nrarp in the chick PSM using in ovo electroporation and analyzed the effect on the dynamic mRNA expression of several cyclic genes. Only embryos with strong green fluorescent protein (GFP) expression in the PSM were used for the analysis (data not shown). After overnight culture the embryos were collected and processed by in situ hybridization. We have previously shown that the electroporation procedure itself using a control plasmid does not affect cyclic gene expression (Dale et al., 2003). Analysis of the embryos electroporated with pCIGNrarp revealed that ectopic Nrarp does not interfere with the normal dynamic patterning of either of the cyclic genes *cLfng* or *cHairy2* ( $n = 16$  and  $n = 12$ ; Fig. 7B,E). In addition, when the electroporated embryos were developed further we observed that ectopic Nrarp did not affect somite formation (data not shown). Thus, our results suggest that misexpression of Nrarp does not interfere with the somitic oscillator. We then examined the effect of blocking cNrarp by electroporation of pRFPRNAiC constructs (Das et al., 2006) designed to generate siRNA-*cNrarp*. We confirmed that these constructs down-regulated the expression of endogenous Nrarp mRNA and protein ( $n = 7$ ; Fig. 6A; data not shown). After electroporation with siRNA-*cNrarp* we similarly observed that *cLfng* and *Hairy2* were not affected in the chick PSM ( $n = 8$  and  $n = 9$ ; Fig. 7C,F). When the embryos were developed further we observed that the treatment did

not affect somite formation (data not shown). Likewise, we performed a similar analysis in the zebrafish embryo by treatment with morpholinos designed to target *nrarp-a* and *nrarp-b* (Ishinati et al., 2005), which did not affect the expression of cyclic gene *her1* in the fish PSM ( $n = 16$  and  $n = 27$ ; Fig. 7H,I). Consistent with these findings, we also found that the expression of the cyclic genes *mLfng* and *mHes7* in homozygous E9.5 *Nrarp*<sup>-/-</sup> mouse embryos was unaffected ( $n = 6$ ; Fig. 7K,M). Together these results indicate that in fish, chick and mouse *Nrarp* function is not critical for the maintenance of the somitogenesis oscillator, and by extension it is also not essential for somite formation.

## DISCUSSION

We report here, the expression of the chick *Nrarp* gene in the early embryo. We performed a more detailed comparative analysis of its expression specifically in the PSM of three vertebrate species: chick, mouse, and zebrafish, and demonstrated that it is a cyclic gene regulated by the Notch signaling pathway. Its expression is also dependent upon Wnt activity in the mouse but not in the chick or fish embryo. We show that the level of *Nrarp* protein does not oscillate in the PSM of the chick embryo, even if *Nrarp* is a cyclic gene regulated by the segmentation clock. Finally, *Nrarp* function does not appear to be essential for the mechanism of the segmentation clock, because interfering with it did not alter the expression of clock genes in embryos of the three species analysed.

We have cloned the chick *Nrarp* homologue and analyzed in detail its expression by in situ hybridization during early development. We have shown that it is expressed in several tissues in which differentiation is known to be regulated by the Notch pathway, including the PSM, the central nervous system and the mesonephric tubules (Fig. 1). A detailed analysis of its expression shows that the expression of *Nrarp* in the PSM of chick and mouse and *nrarp-a* in the PSM of zebrafish embryos of the same stage of development varies with a profile characteristic of a cyclic gene. Our in vitro experiments using the half embryo culture system demonstrate that indeed the different expression profiles observed are due to the dynamic expression of *Nrarp* (Fig. 4E–L). Similar dynamic expression of *mNrarp* has also been reported recently (Sewell et al., 2009). The graphical representation of our analysis of *cNrarp* profile over one full cycle of oscillation shows that the transcripts progression is faster in the caudal PSM than in the medial and rostral regions (Fig. 2L). However, although the pattern is similar to those of other Notch target clock genes analyzed in the same way (Dale et al., 2003; Maroto et al., 2005), there is a major difference localized to the caudal region, because in the case of *cNrarp*, there does not appear to be a distinct and rapid down-regulation of expression caudally as the front of expression moves rostrally. Both *cLfng* and *cHairy1* mRNAs are degraded fairly rapidly in the caudal PSM, with 20–25% and 30–35% of the embryos displaying a caudal domain of expression, respectively. However, *cHairy2* expression is maintained longer in this domain, with 65–70% of the embryos displaying caudal expression (Maroto et al., 2005). *cNrarp* seems to be a still more dramatic situation because it is expressed, at least at a weak level, in the caudal domain of most embryos. The graphical representation summarizes the fact that the transcripts produced by a new cycle seem to overlap with the decaying transcripts from the previous cycle. The situation is quite similar in zebrafish, where the transcripts of *nrarp-a* can be detected in the caudal region long after *deltaC* has been already degraded (Fig. 3).

Once the paraxial mesoderm matures *cNrarp* disappears just before the formation of the new somitic border and is then absent in the somites. This absence of *Nrarp* transcripts in the forming somite of the chick embryo is different in the mouse and zebrafish embryo, where the expression is maintained in the caudal half of the newly formed somite, which indicates that its function could be conserved between different vertebrate embryos along the PSM but not during the formation of the somitic border and in the somite.

The fact that *Nrarp* cycles in synchrony with chick and mouse *Lfng* and zebrafish *deltaC* suggests that it is a Notch-related cyclic gene. Consistent with this idea is the fact that in the absence of Notch activity brought about by treatment with the Notch-blocking drugs or in fish and mouse embryos carrying a mutation in Notch pathway components (Krebs et al., 2001; Sewell et al., 2009; Ferjentsik et al., 2009) the expression of *Nrarp* is severely compromised in the PSM. This Notch dependency is also compatible with the fact that its progression is not abolished in the short term when the sample is cultured in the presence of cycloheximide, as previously shown for other Notch-dependent cycling genes (Palmeirim et al., 1997; McGrew et al., 1998; Leimeister et al., 2000). Sewell et al. (2009) have recently reported that this synchrony of oscillation between *mLfng* and *mNrarp* is different at stage E9.5, when they are not in synchrony, and at stage E10.5, when they are in synchrony. We found, however, their expression in the PSM is in synchrony at both developmental stages. These different interpretations could be due to the difficulty to set the right level of staining between two cyclic genes with different half lives.

It is widely accepted that the Notch and Wnt signaling pathways are responsible for the dynamic expression of several downstream cyclic genes. When we evaluated *Nrarp* dependence with regard to Wnt activity, we found that, whereas the treatment with Wnt-blocking drug CKI-7 abrogates *Nrarp* in the mouse PSM, its expression is maintained in the chick and zebrafish PSM. These findings suggest that the Wnt-dependency of *Nrarp* expression might not be conserved between different vertebrate species. We think these differences could be related with our recent observations regarding the species-specific implication of Wnt in the machinery of the somitic oscillator in the chick and the mouse embryo (Gibb et al., 2009). Thus, homologues of the Wnt target genes that oscillate in the mouse PSM, such as *mAxin2* and *mNkd1*, do not cycle across the chick PSM. In addition, exposure to CKI-7 abolished *mLfng* in the mouse PSM, but a similar treatment only slightly down-regulated *cLfng* in the chick PSM, although this treatment did appear to lengthen the period of oscillations. The regulation of mouse Notch targets by Wnt is likely to be indirect and may possibly invoke one of the previously reported roles for Wnt in the regulation of a Notch signal transduction component, which have as yet not been shown to occur in the PSM. If Wnt is not so relevant for the chick somitic oscillator, then it would make sense that *Nrarp* expression in the PSM, or that of any other cyclic gene, is not severely affected by its absence. Likewise, Wnt may not play a prominent role in the fish clock mechanism, at least judged by the lack of effect of Wnt inhibition on *nrarp-a* expression.

Our data show that *Nrarp* transcripts may be more stable than those of the other clock genes analyzed to date. The comparative analysis of the mRNA degradation rates of *cNrarp* vs. *cLfng* in a timed series after inhibition of Notch signaling highlights this fact; the degradation rate of *cNrarp* mRNA does indeed appear to be more protracted than that of *cLfng* in the PSM (Fig. 6D–G,I–L). *cLfng* expression has already disappeared from this tissue after 2 hr of DAPT treatment at a time when *cNrarp* expression is still widespread in the PSM, albeit reduced in intensity. On the other hand, *cNrarp* in the neural tube appears to be independent of Notch signaling, because it is still strongly expressed in this tissue after 16 hr of exposure to DAPT, whereas *cLfng* is clearly Notch-dependent. Further analysis will be required to reveal the specific regulation of *cNrarp* in the chick neural tube.

The two clock genes analyzed at the protein level, namely the Notch target genes *cLfng* and *mHes7*, displayed a dynamic profile in the PSM similar to that of the mRNA (Dale et al., 2003; Bessho et al., 2003). These patterns are consistent with the expression profile of the intracellular fragment of Notch (NICD) being also dynamic along the PSM (Huppert et al., 2005), which can be interpreted as Notch activity being dynamic along the PSM. The fact that *cLfng* and *mHes7* are expressed with cyclic profile makes sense, because they both negatively regulate transduction of Notch signaling; thus, their periodic absence is crucial in



generating the oscillations (Dale et al., 2003; Bessho et al., 2003). However, that would not necessarily be the case for those proteins whose presence does not impinge on the normal propagation of the oscillator. When we analyzed cNrarp protein levels in the caudal PSM from embryos in different phases of an oscillation, we did not observe variations (Fig. 6B). Consistent with these findings is the fact that after blocking Notch activity the half life of cNrarp protein is significantly longer than that of cLfng (Fig. 6H). The profile of expression of cNrarp in the PSM suggests that, unlike cLfng and mHes7, its continuous presence does not interfere with the somitogenesis oscillator. Indeed, in contrast to the effect we saw with *cLfng* (Dale et al., 2003), we did not observe any effect on cyclic gene expression or somite formation when we ectopically expressed Nrarp in the chick PSM by electroporation. Because it has been reported that morpholino treatment against Nrarp stabilizes NICD (Ishitani et al., 2005), it seemed more likely that its lack of expression could produce an effect consistent with an extended half life of NICD. Surprisingly, we found that, in the absence of Nrarp, cyclic gene expression is unaffected in all three species analyzed. This apparent lack of phenotype is not easy to explain, although it suggests that, even if it is implicated in NICD stability during somitogenesis, Nrarp function might not be a key component in the somitogenesis clock mechanism. Future analysis will help to understand its specific implication in the segmentation process.

## EXPERIMENTAL PROCEDURES

### Embryos and Somite Staging

Fertilized chicken eggs (*Gallus gallus*) purchased from commercial sources (Henry Stewart & Co, Lincolnshire, UK) were incubated for specific periods of time in a humidified atmosphere at 38°C. The embryos were staged according to the developmental table of Hamburger and Hamilton (HH) (Hamburger and Hamilton, 1951) and by counting somite pairs. Wild-type CD1 mice embryos were harvested from timed mated pregnant females between 9.5 and 10.5 days postcoitum (E9.5–E10.5). Wild-type (after eight) *aei/deltaD* mutant and (deadly seven) *des/notch1a* mutant zebrafish embryos were obtained by natural spawnings, raised at 28.5°C and then the stage was determined under the dissecting microscope.

### Embryo Culture

HH stage 11–12 chick embryos and E9.5–E10.5 mouse embryos were isolated, and the caudal portion was divided into two halves by cutting along the neural tube. When required, the explants were cultured on polycarbonate filters (0.8 µM, Millipore) floating on top of culture medium composed of L15 medium (Gibco) supplemented with 10% chick serum, 5% fetal calf serum, 2.5% NaHCO<sub>3</sub>, and 1% penicillin/streptomycin solution (Gibco). At the end of the culture period, the explants were transferred into 4% paraformaldehyde solution, separated from the filter, and then analyzed by in situ hybridization for gene expression. Three different series of experiments were performed, as described previously (Palmeirim et al., 1997; Dale et al., 2003): (A) The two half explants were fixed and stained with different riboprobes. (B) One half explant was fixed and the other half was cultured for 50 and 90 min (chick) or 70 min (mouse). (C) The two halves or two different set of embryos were cultured for different periods of time in the presence or absence of 100 µM DAPT to inhibit Notch activity (Micchelli et al., 2003), 200 µM CKI-7 to inhibit Wnt activity (Peters et al., 1999; McKay et al., 2001; Gibb et al., 2009), or 20 µM cycloheximide or CHX (Sigma) to inhibit protein synthesis. For morpholino treatment, the sequence we used to target *nrarp-a* was 5'-GATGCTTCACACTGGGAGAACTCG-3' and for *nrarp-b* it was 5'-ATGATTTTCAGCAGGTTGACCAAAACG-3', as previously described (Ishitani et al., 2005).

### Whole-Mount In Situ Hybridization

We amplified chick *Nrarp* by RT-PCR from cDNA prepared with embryos HH stage 10–13. We used primers designed from the sequence XM\_428951 posted in NCBI Database, which by the gene prediction method GNOMON corresponds to a putative gene located on chromosome 17 encoding for an ankyrin-repeat protein. Mouse *Nrarp* and zebrafish *nrarp-a* were amplified by PCR with specific primers designed from their sequence, AY046077 and AF509780, respectively. Chick and mouse *Lfng*, chick *Hairy2*, mouse *Hes7*, and zebrafish *her1* and *deltaC* probes were prepared as described (Holley et al., 2000; Jiang et al., 2000; Bessho et al., 2001; Dale et al., 2003, 2006). Whole-mount in situ hybridization was done basically as described (Henrique et al., 1995; Gibb et al., 2009). Images were taken using a Leica MZ16 APO microscope.

### Fluorescent Double In Situ Hybridization

The double in situ hybridization was performed as described (Julich et al., 2005). Zebrafish embryos at approx. the 10-somite stage were stained with the fluorescein-tyramide substrate first. After inactivation of the peroxidase enzyme with 1% H<sub>2</sub>O<sub>2</sub> in 100% methanol, embryos were then analyzed for the Cy3-tyramide substrate. Images were taken using a Zeiss Confocal LSM 510 microscope.

### Graphical Analysis

A large set of stage-matched chick embryos containing 12–17 somites were analyzed by in situ hybridization for expression of chick *Nrarp* (n = 84), similar to the analysis performed for other cyclic genes (Dale et al., 2003, Maroto et al., 2005). Briefly, the domains of expression were measured in each embryo, as was the distance of these domains from the last formed somitic boundary. These values were arranged in order of the advancing limit of the anterior expression limit and then plotted as a graphical representation of the PSM of all the embryos analyzed using Microsoft Excel.

### qRT-PCR

RNA was isolated from the posterior half of PSM using RNeasy micro kit (Qiagen) and a cDNA pool was generated by using ImProm-II RT system (Promega). The PCR reaction was accomplished in the presence of SYBR Green Supermix (Bio-Rad) and the reactions were measured in a Master-cycler ep realplex (Eppendorf) using the following cycling conditions: 95°C for 5 min, 40 cycles at 95°C for 15 sec, and 55°C for 60 sec. Primers to quantify *Nrarp* mRNA levels were designed using Primer3. The two primers used were 5'-ATGAGCCAGAGCGACGTGTCGC-3' and 5'-GCTCCAGGTTGCCGTCGATGAC-3'. Normalization was performed against housekeeping gene *GAPDH* amplified using the primers 5'-TGACCTGCCGTCTGGAGAAACC-3' and 5'-CTATATCCAAACTCATTGTCATACCAGGAAAC-3'.

### Box Plot

For protein ratio, exposed films were scanned after Western blot analysis and densitometric analysis of bands was performed using ImageJ 1.40g software. Density of *Nrarp* band was normalized to the density of appropriate  $\alpha$ -Tubulin band of the same sample to get the relative expression level of *Nrarp* protein in each of them. Relative expression levels of *Nrarp* were plotted in box plot using Sigma-Plot 10.0. The numbers on the vertical axis represent the ratio between the *Nrarp* expression level of each sample and the sample with minimal expression level. Twenty-seven protein samples analyzed in total, relative expression levels were normalized against housekeeping protein  $\alpha$ -Tubulin and then plotted in ratio to minimal value from 1.00 to 1.68. For mRNA ratio, values were obtained by quantitative real-time RT-PCR. Twenty mRNA samples analyzed in total, relative

expression levels were normalized against *GAPDH* and plotted in ratio to minimal value from 1.00 to 15.10. Upon the MWW test, these two set of values are significantly different ( $P = 0.001$ ).

### **Nrarp Antibody and Western Blot Analysis**

Full length chick *Nrarp* was cloned in pGEX to prepare a GST-Nrarp fusion protein, which was expressed in BL21s and purified on GST-Sepharose. The resulting protein was identified by mass spec. analysis. The polyclonal anti-Nrarp antibody (Eurogentec) was affinity purified using cNrarp protein. The polyclonal anti-Lfng antibody (Eurogentec) was prepared using protein prepared as previously reported (Dale et al., 2003). For the analysis of Nrarp and Lfng, protein levels in the PSM embryos were treated independently. The left side of each HH 11–12 embryo was immediately fixed and analyzed by in situ hybridization using a *cLfng* probe to visualize the phase of oscillation in the same embryo. Just the posterior half of the PSM isolated from the right side of the same embryo was dissected in cold PBS containing the Complete cocktail of protease inhibitors (Boehringer Mannheim). This sample was used to run a polyacrylamide gel and then the Western blot analysis was performed using a monoclonal  $\alpha$ -Tubulin antibody (ab7291, Abcam) or the polyclonal anti-Lfng and anti-Nrarp antibodies. Anti-rabbit IgG (Pierce, #31460) and anti-mouse IgG (Pierce, #31430) secondary peroxidase-conjugated polyclonal antibodies were used and the membranes were revealed using ECL (Pierce, #34080).

### **In Ovo Electroporation**

The technique was performed as described previously using plasmids to target the PSM precursor region of HH stage 4–5 chick embryos (Dubrulle et al., 2001; Dale et al., 2003). We used pCIG-Nrarp to ectopically express Nrarp and pRFPRNAiCNrarp(A) (5'-ACCTGATACCAAGGCCAAATA-3') plus pRFPRNAiC-Nrarp(B) (5'-ACGGCAACCTGGAGCTCGTCAA-3') to target the expression of endogenous Nrarp. pRFPRNAiC has been described and validated previously (Das et al., 2006).

### **Acknowledgments**

We thank the J.K.D. and M.M. laboratories for stimulating discussions and Y. Bessho for the discussion of results. We thank the Protein Production and Assay development team (coordinated by H. McLaughlan and J. Hastie) for expression and purification of Nrarp and Lfng. We also thank J. Nguyen and M.L. Dequeant for their help at different moments of the project, and M. Pryde and M. Reilly for their administrative support. Research in the laboratory of Y.J.J. is supported by the Biomedical Research Council of A\*STAR (Agency for Science, Technology and Research), Singapore. Research in the laboratory of S.W. is supported by the BBSRC. Research in the laboratory of O.P. has been supported by Stowers Institute for Medical Research and partly by the NIH. O.P. is a Howard Hughes Medical Institute Investigator. J.K.D. is a Royal Society University Research Fellow and holds an MRC New Investigators Award. M.M. holds an MRC Career Development Award.

Grant sponsor: NIH; Grant number: R01 HD043158; Grant sponsor: MRC; Grant number: Career Developmental Award G120/989.

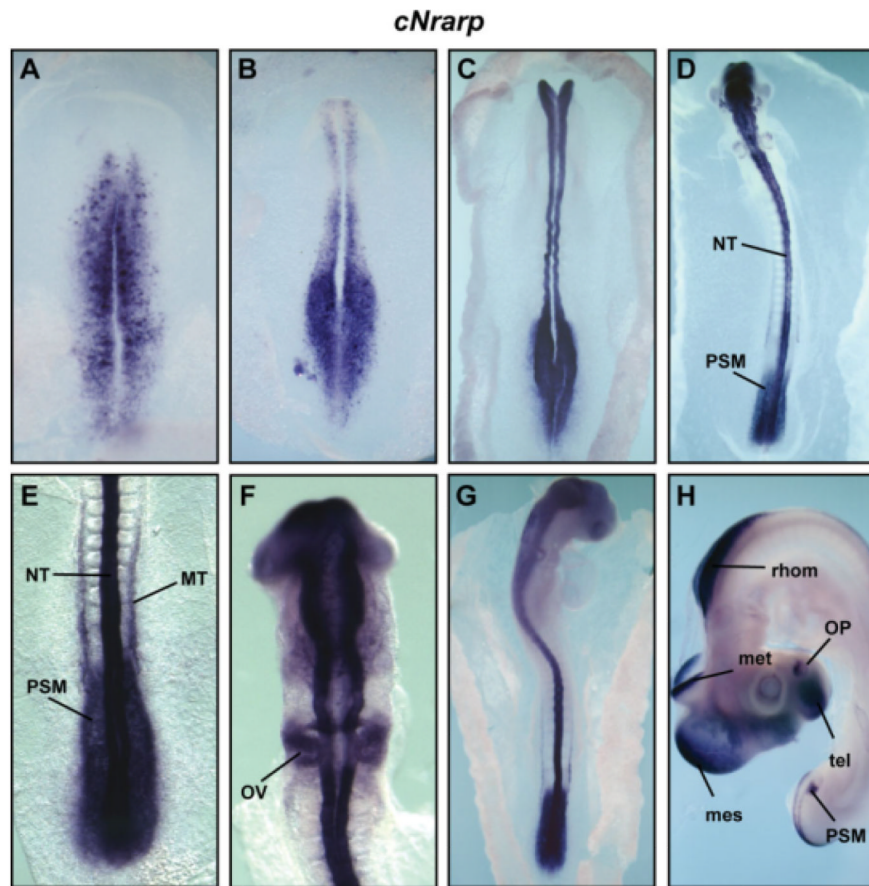
### **REFERENCES**

- Aulehla A, Johnson RL. Dynamic expression of lunatic fringe suggests a link between notch signaling and an autonomous cellular oscillator driving somite segmentation. *Dev Biol.* 1999; 207:49–61. [PubMed: 10049564]
- Aulehla A, Wehrle C, Brand-Saberi B, Kemler R, Gossler A, Kanzler B, Herrmann BG. Wnt3a plays a major role in the segmentation clock controlling somitogenesis. *Dev Cell.* 2003; 4:395–406. [PubMed: 12636920]
- Bellairs, R. The tail bud and cessation of segmentation in the chick embryo. In: Bellairs, E.; Lash, JW., editors. *Somitogenesis in developing embryos.* Plenum Press; New York: 1986. p. 161-178.

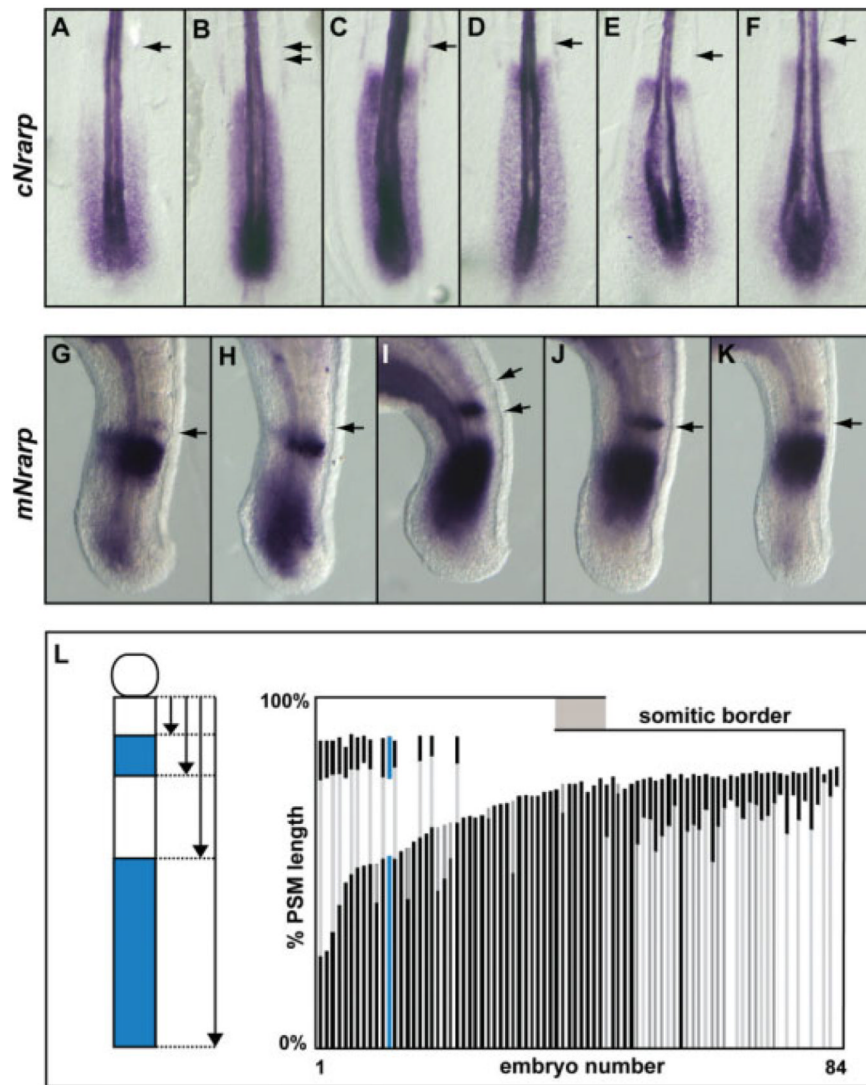
- Bessho Y, Sakata R, Komatsu S, Shiota K, Yamada S, Kageyama R. Dynamic expression and essential functions of *Hes7* in somite segmentation. *Genes Dev.* 2001; 15:2642–2647. [PubMed: 11641270]
- Bessho Y, Hirata H, Masamizu Y, Kageyama R. Periodic repression by the bHLH factor *Hes7* is an essential mechanism for the somite segmentation clock. *Genes Dev.* 2003; 17:1451–1456. [PubMed: 12783854]
- Bryson-Richardson RJ, Currie PD. The genetics of vertebrate myogenesis. *Nat Rev Genet.* 2008; 9:632–646. [PubMed: 18636072]
- Catala M, Teillet MA, Le Douarin NM. Organization and development of the tail bud analyzed with the quail-chick chimera system. *Mech Dev.* 1995; 51:51–65. [PubMed: 7669693]
- Christ B, Huang R, Scaal M. Amniote somite derivatives. *Dev Dyn.* 2007; 236:2382–2396. [PubMed: 17557304]
- Chuai M, Weijer CJ. The mechanisms underlying primitive streak formation in the chick embryo. *Curr Top Dev Biol.* 2008; 81:135–156. [PubMed: 18023726]
- Cinquin O. Understanding the somitogenesis clock: what's missing? *Mech Dev.* 2007; 124:501–517. [PubMed: 17643270]
- Dale JK, Maroto M, Dequeant ML, Malapert P, McGrew M, et al. Periodic Notch inhibition by Lunatic Fringe underlies the chick segmentation clock. *Nature.* 2003; 421:275–278. [PubMed: 12529645]
- Dale JK, Malapert P, Chal J, Vilhais-Neto G, Maroto M, Johnson T, Jayasinghe S, Trainor P, Herrmann B, Pourquié O. Oscillations of the snail genes in the presomitic mesoderm coordinate segmental patterning and morphogenesis in vertebrate somitogenesis. *Dev Cell.* 2006; 10:355–366. [PubMed: 16516838]
- Das RM, Van Hateren NJ, Howell GR, Farrell ER, Bangs FK, Porteous VC, Manning EM, McGrew MJ, Ohyama K, Sacco MA, Halley PA, Sang HM, Storey KG, Placzek M, Tickle C, Nair VK, Wilson SA. A robust system for RNA interference in the chicken using a modified microRNA operon. *Dev Biol.* 2006; 294:554–563. [PubMed: 16574096]
- Dequeant ML, Pourquié O. Segmental patterning of the vertebrate embryonic axis. *Nat Rev Genet.* 2008; 9:370–382. [PubMed: 18414404]
- Dequeant ML, Glynn E, Gaudenz K, Wahl M, Chen J, Mushegian A, Pourquié O. A complex oscillating network of signaling genes underlies the mouse segmentation clock. *Science.* 2006; 314:1595–1598. [PubMed: 17095659]
- Dovey HF, John V, Anderson JP, Chen LZ, de Saint Andrieu P, Fang LY, Freedman SB, Folmer B, Goldbach E, Holsztynska EJ, Hu KL, Johnson-Wood KL, Kennedy SL, Kholodenko D, Knops JE, Latimer LH, Lee M, Liao Z, Lieberburg IM, Motter RN, Mutter LC, Nietz J, Quinn KP, Sacchi KL, Seubert PA, Shopp GM, Thorsett ED, Tung JS, Wu J, Yang S, Yin CT, Schenk DB, May PC, Altstiel LD, Bender MH, Boggs LN, Britton TC, Clemens JC, Czilli DL, Dieckman-McGinty DK, Droste JJ, Fuson KS, Gitter BD, Hyslop PA, Johnstone EM, Li WY, Little SP, Mabry TE, Miller FD, Audia JE. Functional gamma-secretase inhibitors reduce beta-amyloid peptide levels in brain. *J Neurochem.* 2001; 76:173–181. [PubMed: 11145990]
- Dubrulle J, McGrew MJ, Pourquié O. FGF signaling controls somite boundary position and regulates segmentation clock control of spatiotemporal Hox gene activation. *Cell.* 2001; 106:219–232. [PubMed: 11511349]
- Ferjentsik Z, Hayashi S, Dale JK, Bessho Y, Herreman A, De Strooper B, del Monte G, de la Pompa JL, Maroto M. Notch is a critical component of the mouse somitogenesis oscillator and is essential for the formation of the somites. *PLoS Genet.* 2009; 5:e1000662. [PubMed: 19779553]
- Gawantka V, Pollet N, Delius H, Vingron M, Pfister R, Nitsch R, Blumenstock C, Niehrs C. Gene expression screening in *Xenopus* identifies molecular pathways, predicts gene function and provides a global view of embryonic patterning. *Mech Dev.* 1998; 77:95–141. [PubMed: 9831640]
- Gibb S, Zagorska A, Melton K, Tenin G, Vacca I, Trainor P, Maroto M, Dale JK. Interfering with Wnt signalling alters the periodicity of the segmentation clock. *Dev Biol.* 2009; 330:21–31. [PubMed: 19272372]
- Hamburger V, Hamilton HL. A series of normal stages in the development of the chick embryo. *J Morphol.* 1951; 88:49–92. [PubMed: 24539719]

- Henrique D, Adam J, Myat A, Chitnis A, Lewis J, Ish-Horowicz D. Expression of a Delta homologue in prospective neurons in the chick. *Nature*. 1995; 375:787–790. [PubMed: 7596411]
- Holley SA. The genetics and embryology of zebrafish metamerism. *Dev Dyn*. 2007; 236:1422–1449. [PubMed: 17486630]
- Holley SA, Geisler R, Nusslein-Volhard C. Control of her1 expression during zebrafish somitogenesis by a delta-dependent oscillator and an independent wave-front activity. *Genes Dev*. 2000; 14:1678–1690. [PubMed: 10887161]
- Horikawa K, Ishimatsu K, Yoshimoto E, Kondo S, Takeda H. Noise-resistant and synchronized oscillation of the segmentation clock. *Nature*. 2006; 441:719–723. [PubMed: 16760970]
- Huppert SS, Ilagan MX, De Strooper B, Kopan R. Analysis of Notch function in presomitic mesoderm suggests a gamma-secretase-independent role for presenilins in somite differentiation. *Dev Cell*. 2005; 8:677–688. [PubMed: 15866159]
- Ishikawa A, Kitajima S, Takahashi Y, Kokubo H, Kanno J, Inoue T, Saga Y. Mouse Nkd1, a Wnt antagonist, exhibits oscillatory gene expression in the PSM under the control of Notch signaling. *Mech Dev*. 2004; 121:1443–1453. [PubMed: 15511637]
- Ishitani T, Matsumoto K, Chitnis AB, Itoh M. Nrarp functions to modulate neural-crest-cell differentiation by regulating LEF1 protein stability. *Nat Cell Biol*. 2005; 7:1106–1112. [PubMed: 16228014]
- Jiang YJ, Aerne BL, Smithers L, Haddon C, Ish-Horowicz D, Lewis J. Notch signalling and the synchronization of the somite segmentation clock. *Nature*. 2000; 408:475–479. [PubMed: 11100729]
- Jouve C, Palmeirim I, Henrique D, Beckers J, Gossler A, Ish-Horowicz D, Pourquié O. Notch signalling is required for cyclic expression of the hairy-like gene *Hes1* in the presomitic mesoderm. *Development*. 2000; 127:1421–1429. [PubMed: 10704388]
- Julich D, Hwee Lim C, Round J, Nicolaije C, Schroeder J, Davies A, Geisler R, Lewis J, Jiang YJ, Holley SA, Tübingen, 2000 Screen Consortium. Beamter/deltaC and the role of Notch ligands in the zebrafish somite segmentation, hindbrain neurogenesis and hypochord differentiation. *Dev Biol*. 2005; 286:391–404. [PubMed: 16125692]
- Krebs LT, Deftos ML, Bevan MJ, Gridley T. The Nrarp gene encodes an ankyrin-repeat protein that is transcriptionally regulated by the notch signaling pathway. *Dev Biol*. 2001; 238:110–119. [PubMed: 11783997]
- Lamar E, Deblandre G, Wettstein D, Gawantka V, Pollet N, Niehrs C, Kintner C. Nrarp is a novel intra-cellular component of the Notch signaling pathway. *Genes Dev*. 2001; 15:1885–1899. [PubMed: 11485984]
- Lanz TA, Hosley JD, Adams WJ, Merchant KM. Studies of Abeta pharmacodynamics in the brain, cerebrospinal fluid, and plasma in young (plaque-free) Tg2576 mice using the gamma-secretase inhibitor N2-[(2S)-2-(3,5-difluorophenyl)-2-hydroxyethanoyl]-N1-[(7S)-5-methyl-6-oxo-6,7-dihydro-5H-dibenzo[b,d]azepin-7-yl]-L-alaninamide (LY-411575). *J Pharmacol Exp Ther*. 2004; 309:49–55. [PubMed: 14718585]
- Leimeister C, Dale K, Fischer A, Klamt B, Hrabe de Angelis M, Radtke F, McGrew MJ, Pourquié O, Gessler M. Oscillating expression of c-Hey2 in the presomitic mesoderm suggests that the segmentation clock may use combinatorial signaling through multiple interacting bHLH factors. *Dev Biol*. 2000; 227:91–103. [PubMed: 11076679]
- Lewis HD, Perez Revuelta BI, Nadin A, Neduvellil JG, Harrison T, Pollack SJ, Shearman MS. Catalytic site-directed gamma-secretase complex inhibitors do not discriminate pharmacologically between Notch S3 and beta-APP cleavages. *Biochemistry*. 2003; 42:7580–7586. [PubMed: 12809514]
- Mara A, Holley SA. Oscillators and the emergence of tissue organization during zebrafish somitogenesis. *Trends Cell Biol*. 2007; 17:593–599. [PubMed: 17988868]
- Maroto M, Dale JK, Dequeant ML, Petit AC, Pourquié O. Synchronised cycling gene oscillations in presomitic mesoderm cells require cell-cell contact. *Int J Dev Biol*. 2005; 49:309–315. [PubMed: 15906246]

- McGrew MJ, Dale JK, Fraboulet S, Pour-quié O. The lunatic fringe gene is a target of the molecular clock linked to somite segmentation in avian embryos. *Curr Biol.* 1998; 8:979–982. [PubMed: 9742402]
- McKay RM, Peters JM, Graff JM. The casein kinase I family in Wnt signaling. *Dev Biol.* 2001; 235:388–396. [PubMed: 11437445]
- Micchelli CA, Esler WP, Kimberly WT, Jack C, Berezovska O, Kornilova A, Hyman BT, Perrimon N, Wolfe MS. Gamma-secretase/presenilin inhibitors for Alzheimer's disease phenocopy Notch mutations in *Drosophila*. *FASEB J.* 2003; 17:79–81. [PubMed: 12424225]
- Morohashi Y, Kan T, Tominari Y, Fuwa H, Okamura Y, Watanabe N, Sato C, Natsugari H, Fukuyama T, Iwatsubo T, Tomita T. C-terminal fragment of presenilin is the molecular target of a dipeptidic gamma-secretase-specific inhibitor DAPT (N-[N-(3,5-difluorophenacetyl)-L-alanyl]-S-phenylglycine t-butyl ester). *J Biol Chem.* 2006; 281:14670–14676. [PubMed: 16569643]
- Niwa Y, Masamizu Y, Liu T, Nakayama R, Deng CX, Kageyama R. The initiation and propagation of Hes7 oscillation are cooperatively regulated by Fgf and notch signaling in the somite segmentation clock. *Dev Cell.* 2007; 13:298–304. [PubMed: 17681139]
- Oates AC, Ho RK. Hairy/E(spl)-related (Her) genes are central components of the segmentation oscillator and display redundancy with the Delta/Notch signaling pathway in the formation of anterior segmental boundaries in the zebrafish. *Development.* 2002; 129:2929–2946. [PubMed: 12050140]
- Ozbudak EM, Lewis J. Notch signalling synchronizes the zebrafish segmentation clock but is not needed to create somite boundaries. *PLoS Genet.* 2008; 4:e15. [PubMed: 18248098]
- Palmeirim I, Henrique D, Ish-Horowicz D, Pourquié O. Avian hairy gene expression identifies a molecular clock linked to vertebrate segmentation and somitogenesis. *Cell.* 1997; 91:639–648. [PubMed: 9393857]
- Peters JM, McKay RM, McKay JP, Graff JM. Casein kinase I transduces Wnt signals. *Nature.* 1999; 401:345–350. [PubMed: 10517632]
- Pirot P, van Grunsven LA, Marine JC, Huylebroeck D, Bellefroid EJ. Direct regulation of the Nrarp gene promoter by the Notch signaling pathway. *Biochem Biophys Res Commun.* 2004; 322:526–534. [PubMed: 15325262]
- Psychoyos D, Stern CD. Fates and migratory routes of primitive streak cells in the chick embryo. *Development.* 1996; 122:1523–1534. [PubMed: 8625839]
- Riedel-Kruse IH, Muller C, Oates AC. Synchrony dynamics during initiation, failure, and rescue of the segmentation clock. *Science.* 2007; 317:1911–1915. [PubMed: 17702912]
- Sawada K, Aoyama H. Fate maps of the primitive streak in chick and quail embryo: ingression timing of progenitor cells of each rostro-caudal axial level of somites. *Int J Dev Biol.* 1999; 43:809–815. [PubMed: 10707904]
- Schoenwolf GC, Garcia-Martinez V, Dias MS. Mesoderm movement and fate during avian gastrulation and neurulation. *Dev Dyn.* 1992; 193:235–248. [PubMed: 1600242]
- Selleck MA, Stern CD. Fate mapping and cell lineage analysis of Hensen's node in the chick embryo. *Development.* 1991; 112:615–626. [PubMed: 1794328]
- Sewell W, Sparrow DB, Smith AJ, Gonzalez DM, Rappaport EF, Dunwoodie SL, Kusumi K. Cyclical expression of the Notch/Wnt regulator Nrarp requires modulation by Dll3 in somitogenesis. *Dev Biol.* 2009; 329:400–409. [PubMed: 19268448]
- Shankaran SS, Sieger D, Schröter C, Czepe C, Pauly MC, Laplante MA, Becker TS, Oates AC, Gajewski M. Completing the set of h/E(spl) cyclic genes in zebrafish: her12 and her15 reveal novel modes of expression and contribute to the segmentation clock. *Dev Biol.* 2007; 304:615–632. [PubMed: 17274976]
- Shook DR, Keller R. Epithelial type, ingression, blastopore architecture and the evolution of chordate mesoderm morphogenesis. *J Exp Zool B Mol Dev Evol.* 2008; 310:85–110.
- Sieger D, Tautz D, Gajewski M. her11 is involved in the somitogenesis clock in zebrafish. *Dev Genes Evol.* 2004; 214:393–406. [PubMed: 15309634]
- Topczewska JM, Topczewski J, Szostak A, Solnica-Krezel L, Hogan BL. Developmentally regulated expression of two members of the Nrarp family in zebrafish. *Gene Expr Patterns.* 2003; 3:169–171. [PubMed: 12711545]

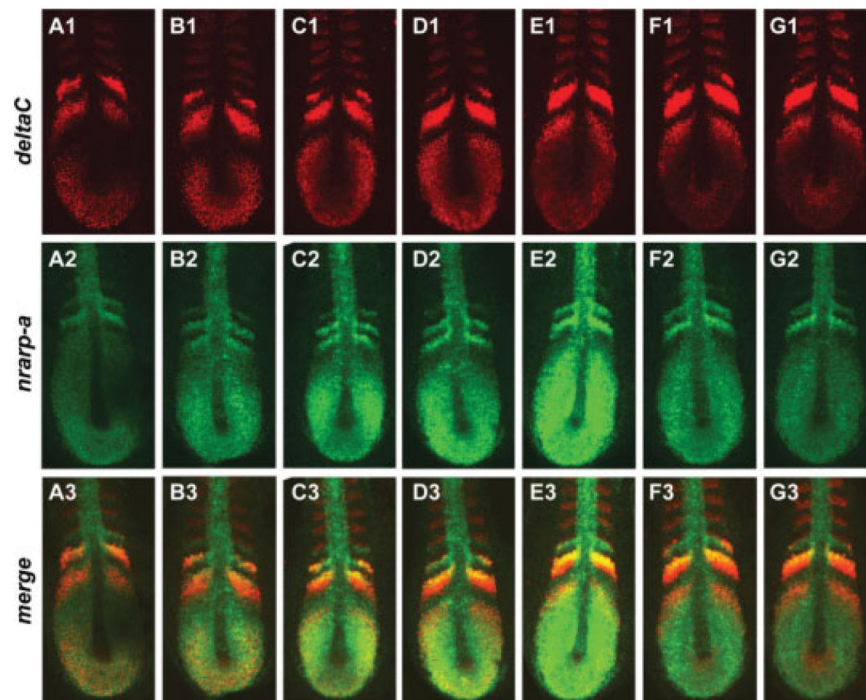


**Fig. 1.** *Nrarp* expression in the early chick embryo. **A–H:** Dorsal view of whole-mount in situ hybridization with a *cNrarp* riboprobe using chick embryos of different stages of development. **A–H:** Hamburger and Hamilton (HH) stage 4 (A), HH stage 7 (B), HH stage 8+ (C), HH stage 12 (D), enlargement of the tail region of a HH stage 13 chick embryo (E), enlargement of the head region of a HH stage 13 chick embryo (F), HH stage 15 (G), and HH stage 21 (H). mes, mesencephalon; met, metencephalon; MT, mesonephric tubules; NT, neural tube; OV, otic vesicles, OP, olfactory pits; PSM, presomitic mesoderm; rhom, rhombencephalon; tel, telencephalon. Rostral is to the top, except in (H) in which the embryos head has turned.

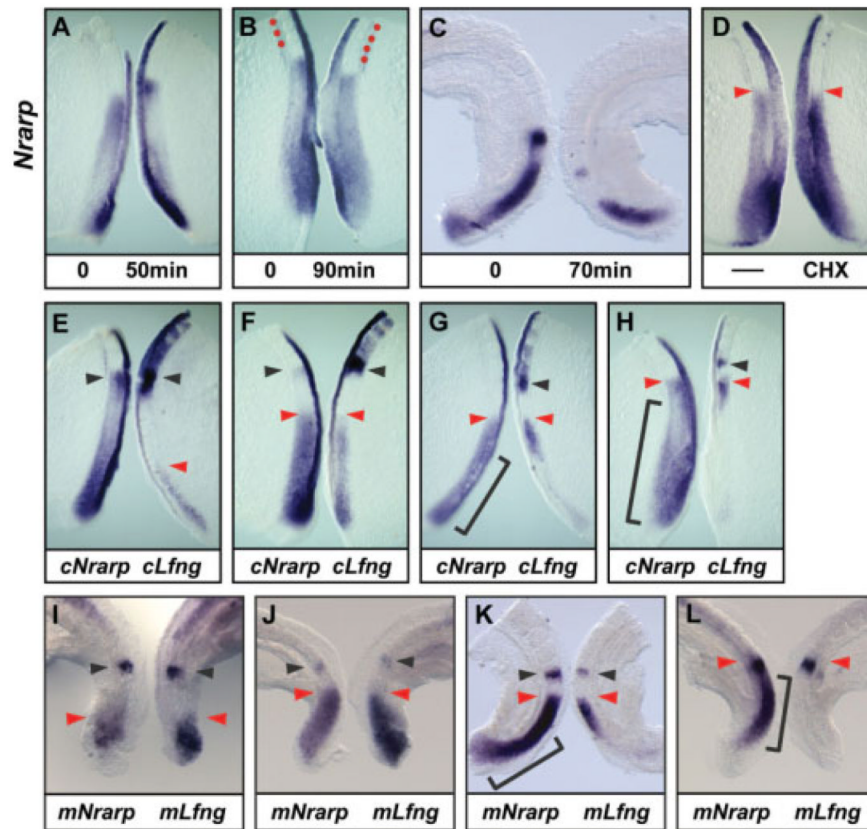


**Fig. 2.** Different patterns of *Nrarp* expression in the chick and mouse presomitic mesoderm (PSM). **A–K:** *Nrarp* expression analyzed by in situ hybridization in the PSM of (A–F) six Hamburger and Hamilton (HH) stage 11–12 chick embryos and (G–K) five E9.5–E10.5 mouse embryos, which display different patterns of expression. The position of the last somitic border is indicated with a black arrow (or two black arrows when the new border is forming). Rostral is to the top. **L:** Graphical analysis of *cNrarp* expression (see the Experimental Procedures section). Each bar along the x-axis represents one embryo. The y-axis represents the extent of gene expression domains along the anteroposterior axis of the PSM, anterior to the top. Darker stripes represent stronger expression domains as compared to lighter bars. The gray rectangle highlights the group of embryos undergoing formation of a new somitic border.

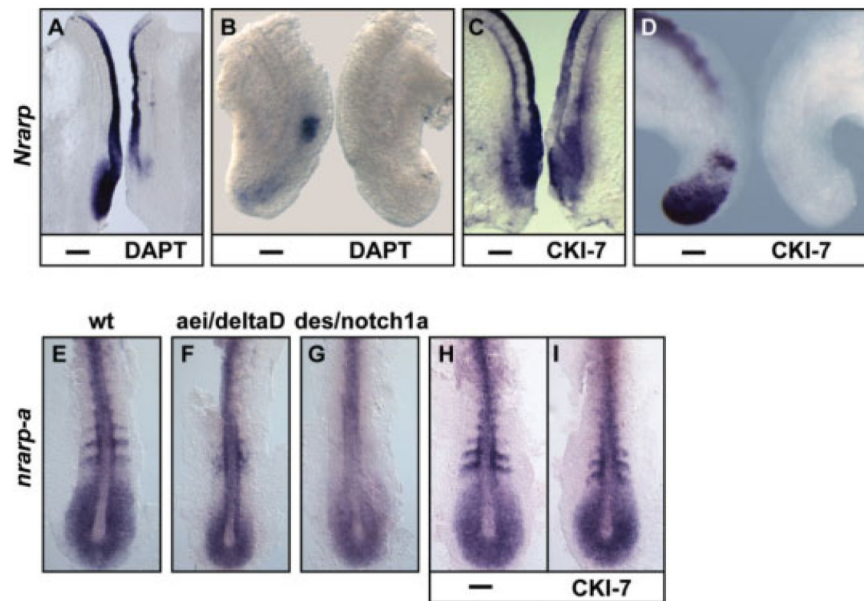




**Fig. 3.** Coexpression of *nrarp-a* and *deltaC* expression in the zebrafish presomitic mesoderm (PSM). **A1–G2:** Fluorescent double in situ hybridization was performed with (A1–G1) Cy3-thyramide substrate to visualize *deltaC* and then (A2–G2) fluorescein-thyramide substrate to visualize *nrarp-a* in the PSM of zebrafish embryos at the 10-somite stage. **A3–G3:** Merge of the two stainings to show that the progression of their expression along the PSM is simultaneous and the major difference in their pattern of expression is due to the longer half life of *nrarp-a* transcripts. Rostral to the top.



**Fig. 4.** *Nrarp* expression is dynamic. A,B,D,E-H: Hamburger and Hamilton (HH) stage 11–12 chick and (C,I–L) embryonic day (E) 9.5 half embryo culture experiments analyzed by in situ hybridization. A–C: One half (left) was fixed immediately and the other half (right) was cultured for 50, 90, and 70 min, respectively. The position of the somites is indicated with red dots. D: Both sides were cultured with or without 20  $\mu$ M cycloheximide. A–D: Both half explants were hybridized with an *Nrarp* probe. E–L: Both sides were fixed and stained with *Nrarp* (left) and *Lfng* (right) to compare their relative patterns of expression during the oscillation. *Nrarp* expression domain lying caudal to that of *cLfng* in the corresponding half embryo is marked with a black bracket, the rostral border of the caudal domain of expression with red arrowheads and the rostral domain of expression with black arrowheads. Rostral to the top.

**Fig. 5.**

*Nrpap* expression is Notch-dependent in fish, chick, and mouse, but Wnt-dependent only in mouse. **A–D:** Hamburger and Hamilton (HH) stage 11–12 chick (A,C) and embryonic day (E) 9.5 (B,D) half embryo culture analysis. Both sides were cultured with or without (A,B) 100  $\mu$ M DAPT to inhibit the Notch activity or (C,D) 200  $\mu$ M CKI-7 to inhibit the Wnt activity. Both half explants were hybridized with an *Nrpap* probe. **E–I:** *nrarp-a* expression analyzed in the PSM of 10-somite stage zebrafish embryos from (E) wild-type (F) *aei/deltaD* mutant, and (G) *des/notch1a* mutant. Zebrafish embryos stained for *nrarp-a* expression after being incubated in the (H) absence or (I) presence of 200  $\mu$ M CKI-7 to inhibit Wnt activity. Rostral to the top.

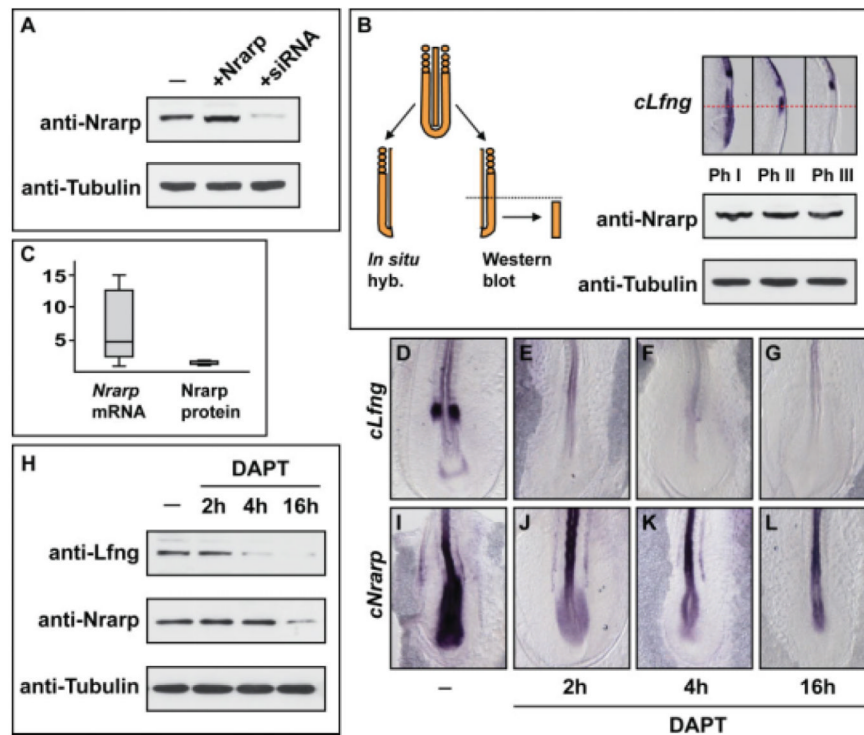


**Fig. 6.** *cNrarp* protein levels do not oscillate in the presomitic mesoderm (PSM) and are more stable than those of *cLfng* after DAPT treatment. **A:** Western blot analysis with anti-Nrarp and anti- $\alpha$ -Tubulin using 50  $\mu$ g of samples prepared from Hamburger and Hamilton (HH) stage 15–16 chick control embryos, embryos electroporated with pCIG-Nrarp to produce ectopic Nrarp or pRFPRNAiC-Nrarp(A+B) to produce siRNA-Nrarp, and incubated overnight. **B:** Western blot analysis of Nrarp protein levels during an oscillation of *cLfng*. Western blots were performed with anti-Nrarp and anti- $\alpha$ -Tubulin using samples prepared with the caudal half of the right isolated PSM of HH stage 11–12 chick embryos from different phases of the oscillation, as shown by the in situ hybridization analysis performed with the left side of the same embryo using *cLfng* probe. **C:** Box plot representation of the differences in the variation of the ratio *Nrarp* mRNA vs. housekeeping *GAPDH* mRNA compared with the variation of the ratio Nrarp protein vs. housekeeping  $\alpha$ -Tubulin protein. Values on the vertical axis represent the ratio between the Nrarp expression level of each sample and the sample with minimal expression level (see the Experimental Procedures section). **D–G, I–L:** HH stage 11–12 chick embryos incubated for different time periods with or without 100  $\mu$ M DAPT to inhibit the Notch activity and then analyzed by in situ hybridization with a *cLfng* (D–G) or an *Nrarp* (I–L) probe. **H:** Western blot analysis of Nrarp and Lfng protein levels in embryos treated with 100  $\mu$ M DAPT for 2, 4, and 16 hr. Western blots were performed with anti-Nrarp, anti-Lfng and anti- $\alpha$ -Tubulin using samples prepared with the caudal half of the right isolated PSM of HH stage 11–12 chick embryos. Rostral to the top.

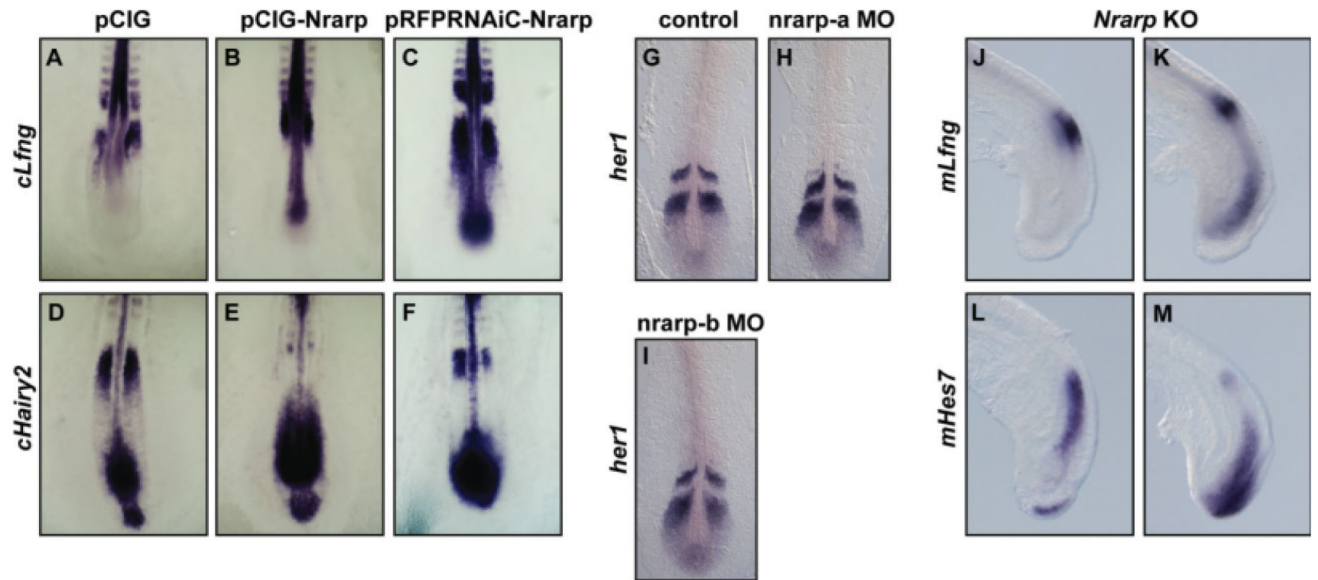


**Fig. 7.**

Gain and Loss of Nrarp function do not affect cyclic gene expression. **A–F:** Electroporated embryos incubated overnight after electroporation with control pCIG (A,D), pCIG-Nrarp (B,E), or pRFPRNAiC-Nrarp(A+B) (C,F), and analyzed by in situ hybridization for *cLfng* (A–C) and *cHairy2* (D–F) expression in the presomitic mesoderm (PSM). **G–I:** Zebrafish embryos at the 10-somite stage after being incubated (G) without treatment (G) or after treatment (H,I) with nrarp-a and nrarp-b morpholinos and then analyzed by in situ hybridization for *her1* expression in the PSM. **J–M:** E9.5 *Nrarp*<sup>-/-</sup> mice embryos analyzed by in situ hybridization for *mLfng* (J,K) and *mHes7* (L,M) expression in the PSM. Rostral to the top.